



Lung fibroblasts promote metastatic colonization through upregulation of stearoyl-CoA desaturase 1 in tumor cells

Guanghua Liu^{1,2,3} · Shi Feng^{1,2,3} · Lin Jia^{1,2,3} · Chunying Wang^{1,2,3} · Yan Fu^{1,2,3} · Yongzhang Luo^{1,2,3}

Received: 1 March 2017 / Revised: 30 October 2017 / Accepted: 7 November 2017
© Macmillan Publishers Limited, part of Springer Nature 2018

Abstract

As a rate-limiting step in metastasis, metastatic colonization requires survival signals from supportive stroma. However, the mechanisms driving this process are incompletely understood. Here, we showed that the proliferation of B16F10 cells was promoted when cocultured with lung fibroblasts. Meanwhile, co-injection of B16F10 tumor cells with mouse lung fibroblasts significantly increased lung metastasis. Based on GEO database, we identified stearoyl-CoA desaturase 1 (SCD1) as a novel factor promoting metastatic colonization. Importantly, we found that fibroblast-secreted cathepsin B (CTSB) induced the upregulation of SCD1 in B16F10 through Annexin A2 (ANXA2) and PI3K/Akt/mTOR pathway. The elevated SCD1 induced a higher ratio of monounsaturated fatty acids to saturated fatty acids in B16F10 cells. The changes in fatty acid composition contributed to tumor cell proliferation and metastatic colonization. Furthermore, targeting SCD1 effectively inhibited lung metastasis and prolonged the overall survival of mice. Meanwhile, the expression of *SCD1* was negatively correlated with disease-free survival in five types of cancer patients. Collectively, our study identifies SCD1 as a critical modulator of tumor cell proliferation that is activated by cathepsin B, secreted by lung fibroblasts at the metastatic niche. Our novel findings provide potential therapeutic targets to prevent tumor metastasis.

Introduction

As one of the most common malignant cancer types, the incidence of melanoma is rising steadily in most Western countries [1, 2]. Despite surgical resection that leads to a good prognosis in the early stages of melanoma, the majority of melanoma patients dies from secondary metastasis, which has a very poor prognosis [2]. However, there are not enough drugs targeting melanoma metastasis due to

a poor understanding of the mechanisms controlling this clinically important process.

Metastasis is a highly inefficient process. Tumor cells have to overcome many obstacles in the process of metastatic cascade, among which organ colonization is regarded as the most complicated and rate-limiting step, because tumor cells need to face the challenges of lack of survival signals and supportive stroma after the arrival at distant organs [3]. Meanwhile, several studies have proved that the interactions between tumor cells and stromal cells at distant organs promote metastatic colonization. Malanchi and colleagues found that stromal fibroblasts contribute to metastatic colonization through the expression of periostin, which recruits Wnt ligands and increases Wnt signaling in cancer stem cells [4]. Massagué's group demonstrated that the binding of macrophage to receptor VCAM-1 can induce survival signals in breast cancer cells infiltrated in the lung [5]. Wculek and Malanchi also found that neutrophil-derived leukotrienes specifically support metastatic initiation [6]. The data from Ahmed's lab showed that adipocytes accelerate ovarian cancer omental metastasis through the activation of SIK2, which drives cancer cells survival and fatty acid oxidation [7].

G. Liu and S. Feng contributed equally to this work.

Electronic supplementary material The online version of this article (<https://doi.org/10.1038/s41388-017-0062-6>) contains supplementary material, which is available to authorized users.

✉ Yongzhang Luo
yluo@mail.tsinghua.edu.cn

¹ The National Engineering Laboratory for Anti-Tumor Protein Therapeutics, Tsinghua University, Beijing, China

² Beijing Key Laboratory for Protein Therapeutics, Tsinghua University, Beijing, China

³ Cancer Biology Laboratory, School of Life Sciences, Tsinghua University, Beijing, China

Fibroblasts are regarded as prominent modifiers in the malignant progression of cancer. The important functions of fibroblasts in the primary tumor microenvironment are well studied, including remodeling of the extracellular matrix, mediating the immune reprogramming and promoting cancer cell survival, metastasis and drug resistance [8]. However, the relationship between fibroblasts and metastatic colonization in secondary organs is poorly established.

Understanding the mechanisms by which fibroblasts promote metastatic colonization will provide the foundation for the development of novel and refined approaches to target metastasis. The purpose of this study was to understand the role of lung fibroblasts (LF) in mediating metastatic colonization and the mechanisms by which this process occurs. Here, we identified stearoyl-CoA desaturase 1 (SCD1) as a key factor to promote metastatic colonization. Cathepsin B (CTSB) secreted by fibroblasts induced the activation of PI3K/Akt/mTOR pathway, resulting in the upregulation of SCD1 in tumor cells. Increased SCD1 expression finally influenced fatty acid composition and cancer cell proliferation. Moreover, targeting SCD1 significantly inhibited lung metastatic colonization by 63.8% and prolonged the median survival time by 22.6%.

Results

LF promote melanoma tumor cell proliferation and metastatic colonization

In order to understand the crosstalk between tumor cells and LF, we first isolated primary murine LF from C57BL/6 mice and conducted a coculture experiment using Millicell hanging cell culture inserts (1 μ m pore size) (Supplementary Figure S1a and b). The results showed that the proliferation of B16F10 tumor cells was significantly increased when cocultured with freshly isolated LF (Fig. 1a). Similarly, the conditioned medium from B16F10-LF coculture system also enhanced the proliferation of B16F10 cells compared to B16F10-CM (Fig. 1b). Then B16F10-GFP cells were mixed with LF in different ratios. We found that the proliferation of B16F10-GFP cells was elevated with the increase in the ratio of LF (Fig. 1c and Supplementary Figure S1c). On the other hand, compared to the B16F10-CM, the rate of apoptosis decreased when tumor cells were treated with the CM from the coculture system (Supplementary Figure S1d).

To confirm the tumor-promoting effect of LF in human cell lines, we cocultured A875 or A375 with human LF MRC5. The results showed that the proliferation of A875 or A375 cells was significantly elevated when cocultured with

MRC5 (Fig. 1d, e). Similarly, the conditioned medium from A875-MRC5 or A375-MRC5 coculture system both enhanced the proliferation (Fig. 1f and g) and decreased the apoptosis rate (Supplementary Figure S1e and f) of A875 or A375 cells, respectively.

To determine whether LF promote metastatic colonization *in vivo*, we intravenously injected B16F10 tumor cells, alone or mixed with freshly isolated LF, into the tail vein of mice. Consistently, the co-injection of LF significantly increased the lung metastasis area compared with the control group (Fig. 1h, i). Similarly, co-injection of A375 with MRC5 increased the number of lung metastasis foci in nude mice (Fig. 1j, k). To confirm the extravasation of freshly isolated LF to the lung, we intravenously injected B16F10 tumor cells alone or mixed with freshly isolated GFP-labeled LF from GFP transgenic mice. We detected the GFP signaling when B16F10 cells were injected with LF but not in the control group (Supplementary Figure S1g), which proved that freshly isolated LF can home and remain in the lung. Taken together, these data demonstrate that LF play an important role in tumor metastatic colonization.

The expression of SCD1 is elevated in B16F10 cells cocultured with LF

We next investigated the mechanism by which LF stimulate the proliferation of B16F10 tumor cells. We analyzed six gene expression profiles (GSE7929, GSE7956, GSE8401, GSE12391, GSE46517, and GSE7553) from GEO datasets, which compared gene expression changes between primary melanoma and metastatic melanoma. We screened out the upregulated genes in metastatic melanoma compared with primary melanoma with the limitation of *P* values less than 0.01. Then, the occurrence frequency for each gene among the six gene expression profiles was analyzed (Supplementary Table 2). We found that only two genes appeared in five datasets, and 40 genes appeared in four datasets. To expand the range of screening, we further analyzed the genes that appeared in three datasets using cBioPortal and selected the genes which were correlated with disease-free survival (DFS) in skin cutaneous melanoma (Fig. 2a). Then, we analyzed the expression of those genes in B16F10 tumor cells cocultured with LF using the method of quantitative real-time PCR (qRT-PCR) (Fig. 2b), and picked up the upregulated ones for western blots validation (Fig. 2c). As shown in Fig. 2c, the expression of SCD1 was elevated most significantly in B16F10 cells when cocultured with LF. The expression levels of SCD1 and its transcriptional factor SREBP1 were also increased in A875 and A375 cells when cocultured with MRC5 (Fig. 2d, e). We also found that the expression level of SCD1 was higher in malignant cell lines, such as B16F10 and A375 than that in murine and

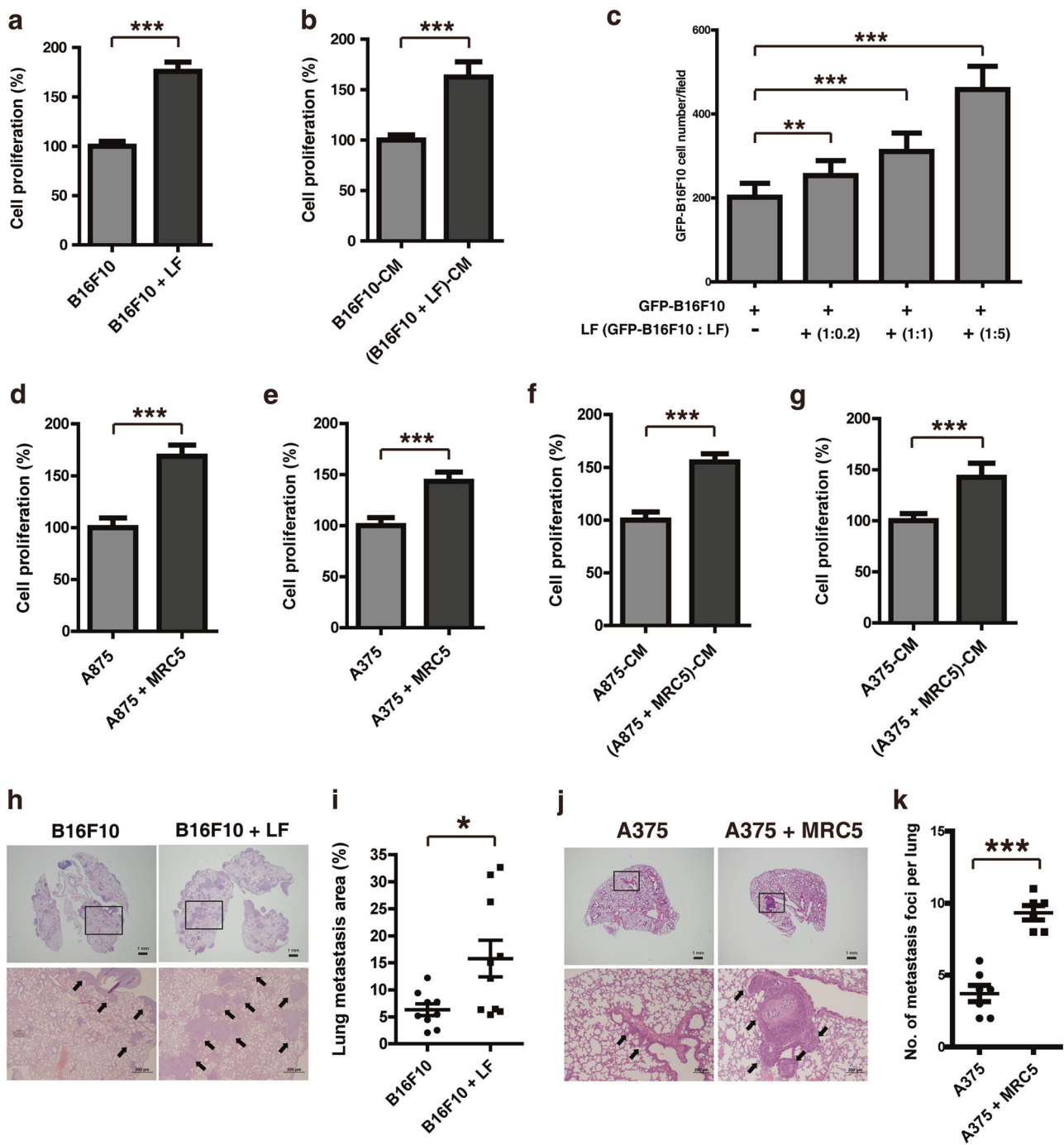
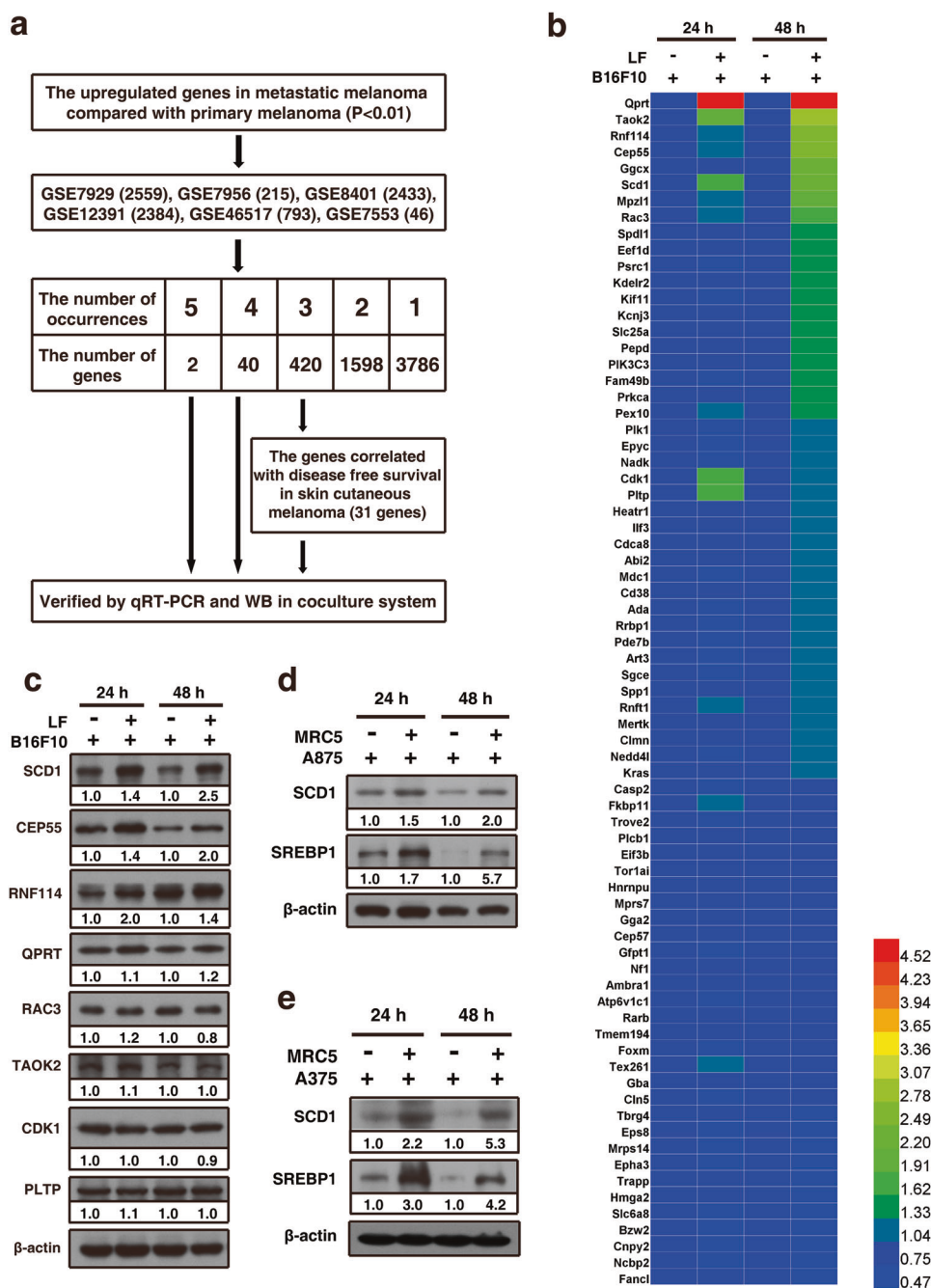


Fig. 1 Lung fibroblasts promote melanoma tumor cell proliferation and metastatic colonization. **a** B16F10 cells were cocultured with freshly isolated lung fibroblasts (ratio, 1:1) and cell proliferation of B16F10 was analyzed with Cell Counting Kit-8. **b** Cell proliferation assay of B16F10 cells treated with conditioned medium (CM) from coculture system. **c** GFP-B16F10 cells were cocultured with lung fibroblasts with different ratio (1:0.2, 1:1, 1:5), and the GFP-positive B16F10 cell population was counted. **d** and **e** A875 cells and A375 cells were cocultured with MRC5 (ratio, 1:5) and cell proliferation of A875 and A375 were analyzed with Cell Counting Kit-8. **f** and **g** Cell proliferation assay of A875 and A375 cells treated with conditioned medium (CM) from A875-MRC5 or A375-MRC5 coculture system. **h**

Mice were intravenously injected B16F10 cells with or without freshly isolated lung fibroblasts (1:1). Lung metastases (metastatic foci; arrows) were detected with HE staining 21 days later ($n = 9$ or 10 /group), scale bars = 1 mm (top). Images were taken at $\times 40$ original magnification (bottom), scale bars = 500 μm (bottom). **i** The percentage of lung metastasis area to total lung area in **h**. **j** Mice were intravenously injected A375 cells with or without MRC5 (1:1). Lung metastases (metastatic foci; arrows) were detected with HE staining 49 days later ($n = 6$ or 7 /group), scale bars = 1 mm (top). Images were taken at $\times 100$ original magnification (bottom), scale bars = 200 μm (bottom). **k** The number of metastasis foci in **j**. * $P < 0.05$, ** $P < 0.01$, *** $P < 0.001$

Fig. 2 The identification of tumor-promoting factors in coculture systems. **a** Schematic representation of the experimental design which showed the identification of tumor-promoting factors in B16F10 cells cocultured with lung fibroblasts. **b** B16F10 cells were cocultured with lung fibroblasts for 24 or 48 h, heat map diagrams of gene expression changes detected by qRT-PCR analysis of interested genes. **c** Immunoblotting of the selected tumor-promoting factors in B16F10 cells that cocultured with lung fibroblasts for 24 or 48 h. **d** and **e** A875 and A375 cells were cocultured with MRC5 for 24 or 48 h, the expression of SCD1 and its transcriptional factor SREBP1 were detected by western blot; β -actin served as loading controls



human fibroblasts (Supplementary Figure S2a). Then, we detected the expression of SCD1 in lung metastatic colonies. As shown in Supplementary Figures S2d and e, the expression of SCD1 was elevated when B16F10 cells were injected with LF. Meanwhile, the expression of SCD1 was positively correlated with the expression of the proliferation marker PCNA (Supplementary Figures S2d and e). Interestingly, the nearby regions of PCNA or SCD1 positive tumor cells were surrounded by activated LF which were α -SMA positive (Supplementary Figures S2f–i). As a central

enzyme in lipid metabolism, SCD1 catalyzes the synthesis of monounsaturated fatty acids (MUFAs) from saturated fatty acids (SFAs) [9]. Recent studies have proved that the expression of SCD1 contributes to tumor cell proliferation and tumorigenesis in many human cancers including prostate, bladder, breast, lung, and clear cell renal cell carcinoma [10–15]. However, the role of SCD1 in the metastatic sites is not well-known. Interestingly, our data reveal that SCD1 may play an important role in lung metastatic colonization.

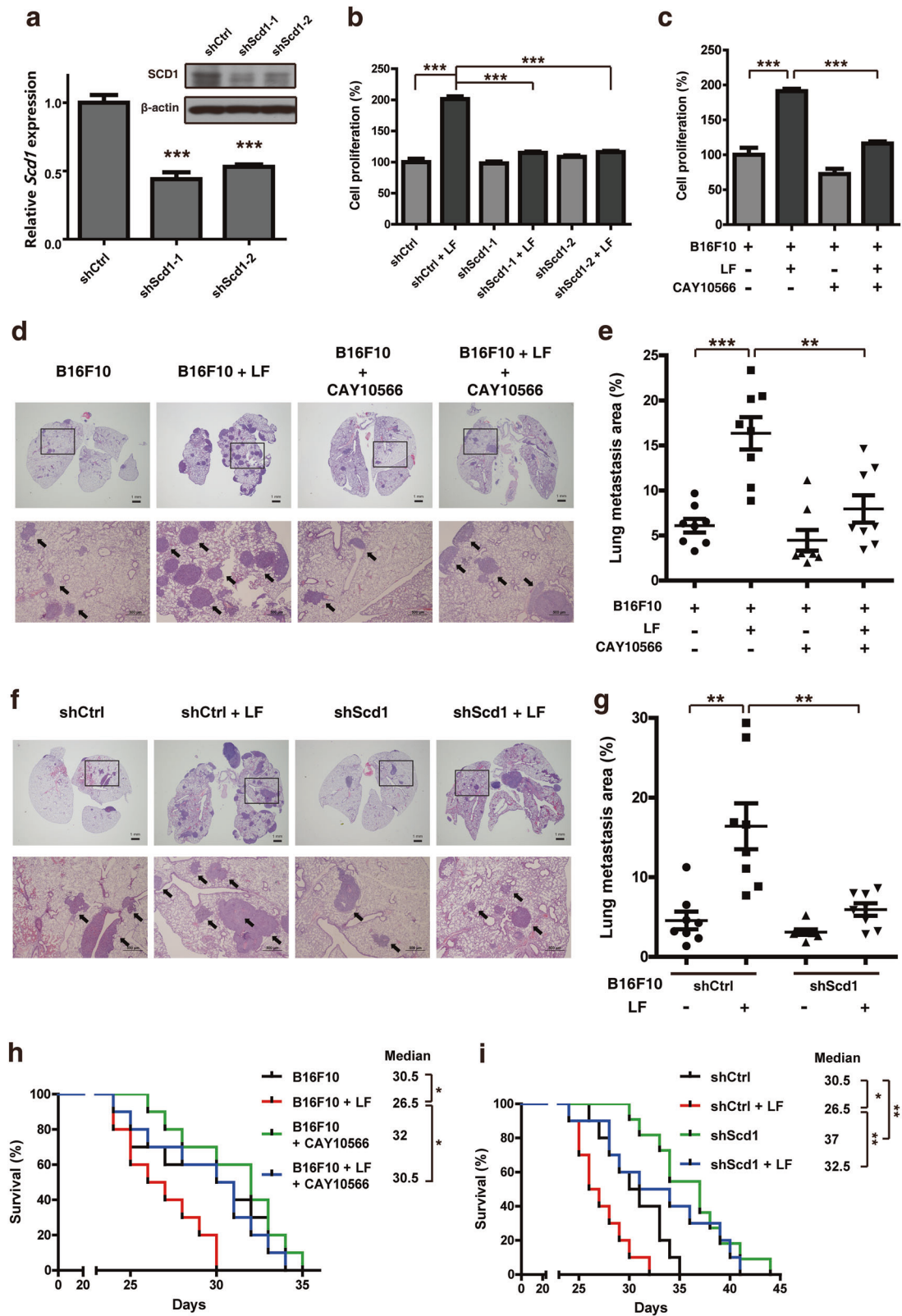


Fig. 3 SCD1 is required for the tumor-promoting effect of lung fibroblasts. **a** The *Scd1* knockdown efficiency was evaluated by qRT-PCR and western blot. **b** B16F10 or *Scd1* knockdown cells were cocultured with lung fibroblasts and cell proliferation was analyzed with Cell Counting Kit-8. **c** Cell proliferation assay of B16F10 cells cocultured with lung fibroblasts or treated with CAY10566. **d** Mice were intravenously injected B16F10 cells with lung fibroblasts or treated with CAY10566. Lung metastases (metastatic foci; arrows) were detected with HE staining 21 days later ($n = 8/\text{group}$), scale bars = 1 mm (top). Images were taken at $\times 40$ original magnification (bottom), scale bars = 500 μm (bottom). **e** The percentage of lung metastasis area to total lung area in **d**. **f** Mice were intravenously injected *Scd1* knockdown cells with or without lung fibroblasts. Lung metastases (metastatic foci; arrows) were detected with HE staining 21 days later ($n = 8/\text{group}$), scale bars = 1 mm (top). Images were taken at $\times 40$ original magnification (bottom), scale bars = 500 μm (bottom). **g** The percentage of lung metastasis area to total lung area in **f**. **h** Kaplan–Meier survival analysis of mice treated the same as described in **d**, ($n = 10/\text{group}$). **i** Kaplan–Meier survival analysis of mice treated with the same as described in **f** ($n = 10$ or $11/\text{group}$). * $P < 0.05$, ** $P < 0.01$, *** $P < 0.001$

SCD1 mediates the tumor-promoting effects of LF

To determine whether SCD1 is required for lung fibroblast-induced growth stimulation of tumor cells, we first generated B16F10 cell lines stably expressing short hairpin RNAs (shRNAs) targeting *Scd1*. The cell lines showed a substantial reduction in the expression of SCD1 both at mRNA and protein levels (Fig. 3a). As shown in Fig. 3b, LF significantly increased the proliferation of B16F10 cells, while targeted depletion of *Scd1* compromised the lung fibroblast-mediated increase of cancer cell proliferation. CAY10566 is a potent and selective chemical inhibitor of SCD1, and the treatment of CAY10566 also reversed the lung fibroblast-induced growth-promoting effect on tumor cells in two coculture systems (Fig. 3c and Supplementary Figure S3a).

Furthermore, we stably overexpressed SCD1 in B16F10 cells (Supplementary Figures S3b and c). Overexpression of SCD1 accelerated the cell proliferation rate and tumor volume compared with controls (Supplementary Figures

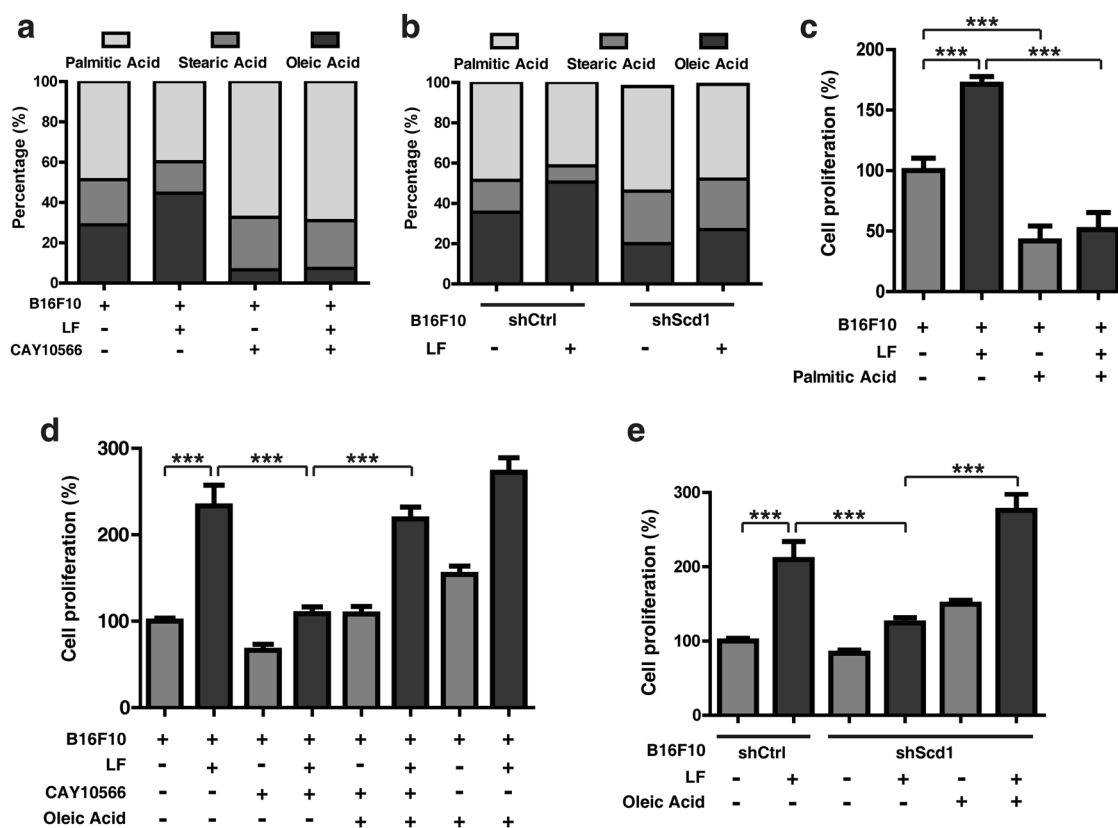


Fig. 4 Lung fibroblasts change the fatty acid composition and induce the activation of PI3K/Akt/mTOR pathway in tumor cells. **a** B16F10 cells were cocultured with lung fibroblasts or treated with CAY10566 for 48 h. Lipid extracts were prepared and analyzed by GC–MS. **b** *Scd1* knockdown cells or vehicle control were cocultured with lung fibroblasts for 48 h. Lipid extracts were prepared and analyzed by

GC–MS. **c** Cell proliferation assay of B16F10 cells cocultured with lung fibroblasts or treated with palmitic acid. **d** Cell proliferation assay of B16F10 cells cocultured with lung fibroblasts or treated with CAY10566 and oleic acid. **e** Cell proliferation assay of *Scd1* knockdown cells cocultured with lung fibroblasts or treated with oleic acid. *** $P < 0.001$

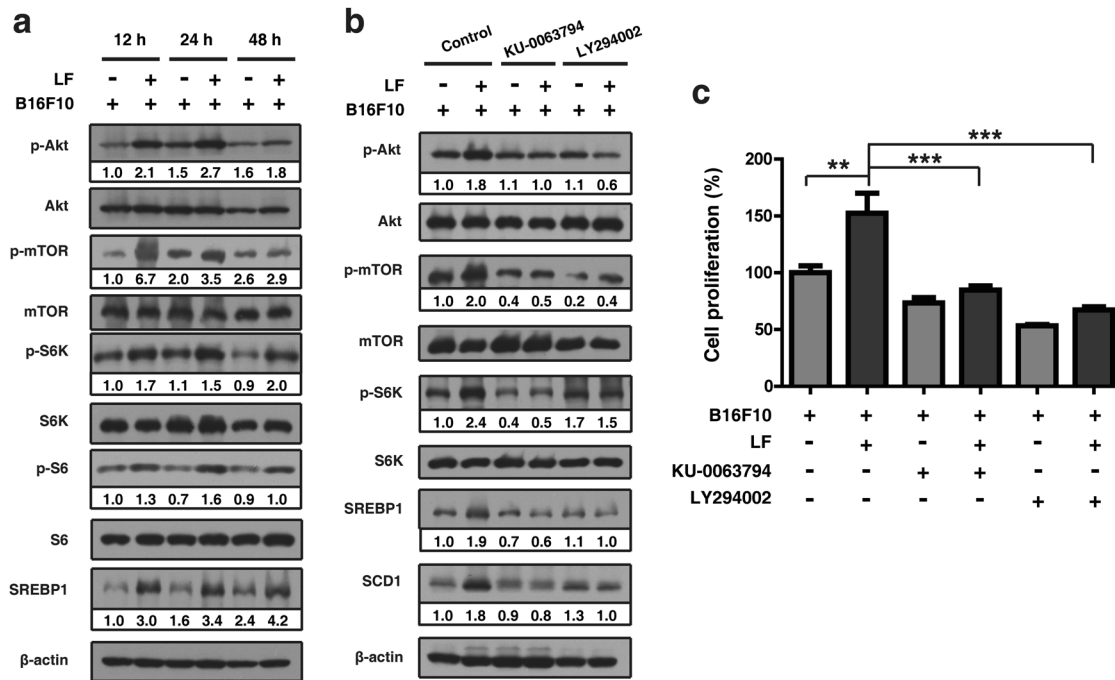


Fig. 5 Lung fibroblasts induce SCD1 expression in tumor cells through the activation of PI3K/Akt/mTOR pathway. **a** B16F10 cells were cocultured with lung fibroblasts for 12, 24, or 48 h and protein lysates were collected for immunoblotting using the indicated antibodies. **b** B16F10 cells were cocultured with lung fibroblasts or treated with KU-

0063794 or LY294002 for 24 h and protein lysates were collected for immunoblotting using the indicated antibodies. **c** Cell proliferation assay of B16F10 cells cocultured with lung fibroblasts or treated with KU-0063794 or LY294002. ** $P < 0.01$, *** $P < 0.001$

S3d and e). In addition, same as the co-injection of B16F10 cells with LF, intravenous injection of SCD1 over-expressing cells significantly elevated the number of lung metastasis foci (Supplementary Figures S3f and g).

To further confirm the role of SCD1 in promoting lung metastatic colonization, we investigated the effect of CAY10566 on metastasis. First, tumor cells alone or with LF were intravenously injected into mice. Then, the mice were treated with CAY10566 once daily for 7 days, and lung metastasis was detected 21 days after tumor cell injection. Similarly, the co-injection of LF increased lung metastasis, while the treatment of CAY10566 significantly compromised lung fibroblast-induced metastasis (Fig. 3d, e). Next, we detected lung metastasis after intravenous injection of shScd1 B16F10 cells alone or mixed with LF. The results showed that targeted depletion of *Scd1* significantly attenuated lung fibroblast-induced metastasis (Fig. 3f, g). Furthermore, monitoring of animal survival revealed that co-injection of B16F10 and LF reduced the median survival time of mice ($P = 0.028$, Fig. 3h). On the other hand, targeted depletion of *Scd1* or the treatment of CAY10566 significantly prolonged the median survival time ($P = 0.022$, Fig. 3h; $P = 0.007$, Fig. 3i, respectively).

Taken together, these data strongly suggest that SCD1 plays a very important role in lung metastatic colonization,

and targeting SCD1 holds great promise in preventing tumor metastasis.

LF promote tumor cell proliferation by changing fatty acid composition

Given the key role of SCD1 in fatty acid metabolism, the above data implied a possible SCD1-driven mechanism by which fatty acid composition influences metastatic colonization. To test this hypothesis, we detected the fatty acid composition in B16F10 cells cocultured with LF. The ratio of MUFA/SFA was increased when B16F10 cells were cocultured with LF (Fig. 4a). Meanwhile, the treatment of CAY10566 and targeted depletion of *Scd1* decreased the ratio of MUFA/SFA both when B16F10 was cultured alone and cocultured with LF (Fig. 4a, b). As SCD1 mainly catalyzes SFAs to MUFAs, we investigated whether the treatment of SFA (palmitic acid) and MUFA (oleic acid) could influence the lung fibroblast-induced growth-promoting effect on tumor cells. As shown in Fig. 4c, palmitic acid inhibited the proliferation of B16F10 cells, and also compromised the lung fibroblast-enhanced tumor cell proliferation. Meanwhile, the addition of oleic acid facilitated the proliferation of B16F10 cells and also rescued the proliferative capacity of B16F10 cells that was inhibited by CAY10566 (Fig. 4d) or targeted depletion of *Scd1* (Fig. 4e).

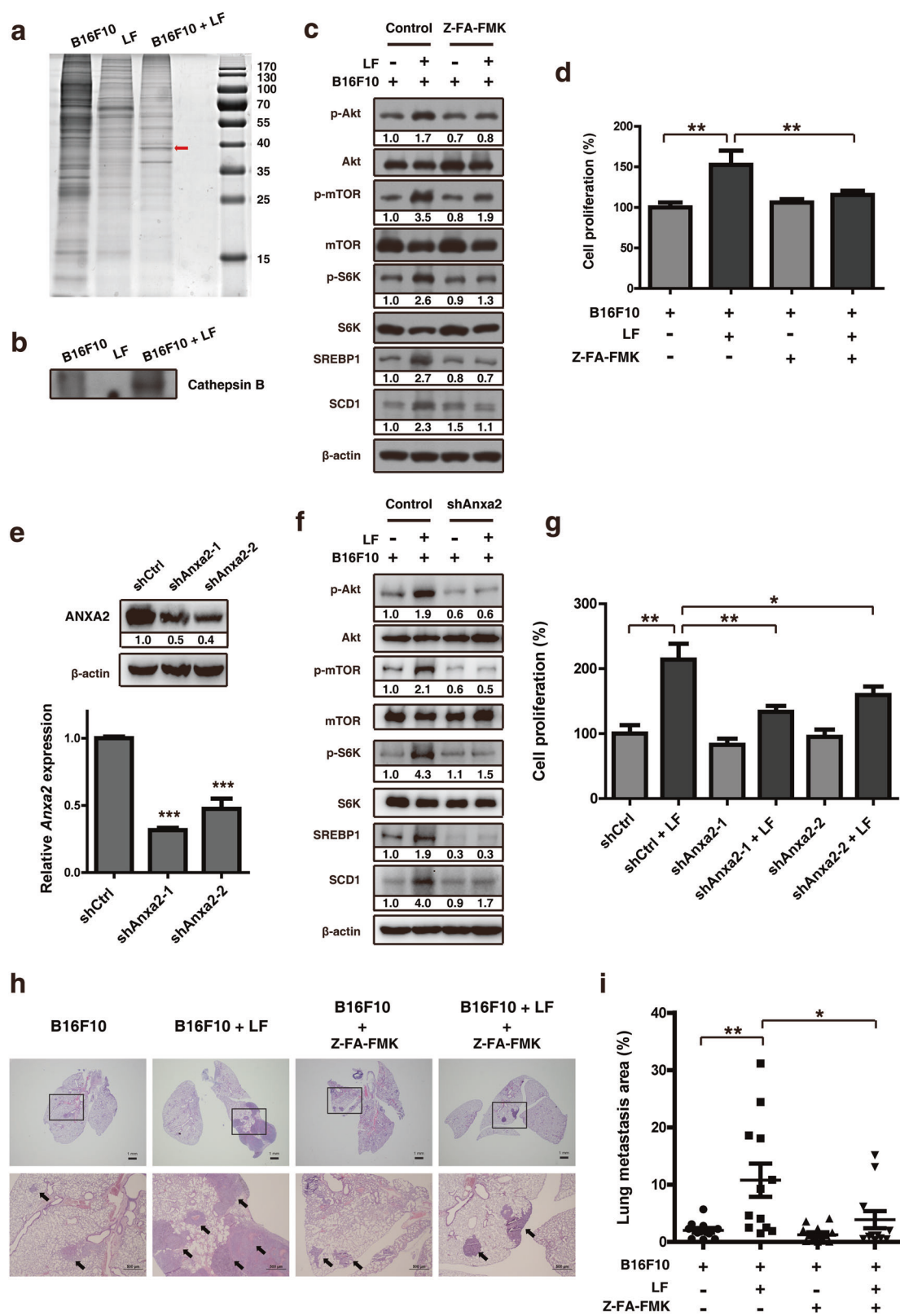


Fig. 6 Lung fibroblast-secreted cathepsin B induces the expression of SCD1 in tumor cells. **a** Conditioned medium from B16F10, lung fibroblasts, or B16F10-CM-treated lung fibroblasts were run on an SDS-PAGE gel and stained with Coomassie blue. The protein band (red arrow) was identified as cathepsin B by liquid chromatography–tandem mass spectrometry. **b** Western blot of cathepsin B in CM from B16F10, lung fibroblasts, or B16F10-CM-treated lung fibroblasts. Equal protein was run on a SDS-PAGE gel, transferred to PVDF membrane and immunoblotted with cathepsin B antibody. **c** B16F10 cells were cocultured with lung fibroblasts and treated with Z-FA-FMK for 24 h, then lysates were collected and immunoblotting performed using the indicated antibodies. **d** Cell proliferation assay of B16F10 cells cocultured with lung fibroblasts or treated with Z-FA-FMK. **e** The *Anxa2* knockdown efficiency was evaluated by qRT-PCR and western blot. **f** B16F10 cells were cocultured with lung fibroblasts and treated with shRNA targeting *Anxa2* for 24 h, then lysates were collected and immunoblotting performed using the indicated antibodies. **g** Cell proliferation assay of B16F10 cells cocultured with lung fibroblasts or treated with shRNAs targeting *Anxa2*. **h** Mice were intravenously injected B16F10 cells with lung fibroblasts or treated with Z-FA-FMK. Lung metastases (metastatic foci; arrows) were detected with HE staining 21 days later ($n = 6/\text{group}$), scale bars = 1 mm (top). Images were taken at $\times 40$ original magnification (bottom), scale bars = 500 μm (bottom). **i** The percentage of lung metastasis area to total lung area in **h**. * $P < 0.05$, ** $P < 0.01$, *** $P < 0.001$

These observations demonstrate that LF increase tumor cell proliferation mainly through the influence on fatty acid composition.

LF induce SCD1 expression in tumor cells by the activation of PI3K/Akt/mTOR pathway

Next, we investigated which pathway mediated the lung fibroblast-induced SCD1 expression in tumor cells. Mammalian target of rapamycin (mTOR) plays critical roles in cell metabolism and cancer progression [16]. As previous studies reported, the expression of SCD1 is also regulated by mTOR pathway [17]. We therefore determined whether LF promoted the expression of SCD1 in tumor cells through activating the PI3K/Akt/mTOR pathway. We performed western blots to examine the phosphorylation status of Akt and mTOR. The results showed that Akt and mTOR were significantly activated in B16F10 tumor cells cocultured with LF (Fig. 5a). As a direct substrate of the mTOR kinase, the phosphorylation level of S6 kinase (S6K) was elevated. The phosphorylation of ribosomal protein S6, the substrate of S6K, was also significantly increased. It is well established that the expression of SCD1 is regulated by SREBP transcription factor family [18], which can be stimulated by S6K. In our study, we also found that LF promoted the expression of SREBP1 in B16F10 tumor cells (Fig. 5a). These results show that the PI3K/Akt/mTOR pathway is activated in B16F10 tumor cells cocultured with LF.

To confirm the involvement of PI3K/Akt/mTOR pathway in the fibroblast-induced SCD1 expression, we treated

B16F10 cells with PI3K inhibitor LY294002 or mTOR inhibitor KU-0063794 in coculture system. Both of them blunted fibroblast-induced activation of PI3K/Akt/mTOR pathway, as assessed by the phosphorylation of Akt, mTOR, and S6K, respectively. Coordinately, the expression of SCD1 and its transcription factor SREBP1 was diminished significantly by both inhibitors (Fig. 5b). The treatment of LY294002 or KU-0063794 also reversed lung fibroblast-mediated increase of tumor cell proliferation (Fig. 5c). Importantly, the addition of oleic acid also partially rescued the proliferative capacity of B16F10 cells that inhibited by KU-0063794 or LY294002 (Supplementary Figure S4). Taken together, the above data confirm that LF indeed induce SCD1 expression in tumor cells through the activation of PI3K/Akt/mTOR pathway.

Lung fibroblast-secreted CTSB induces the expression of SCD1 in tumor cells

To gain insight into how LF promotes proliferation of tumor cells, we studied the lung fibroblast-secreted factors using tandem mass spectrometry by analyzing the secretome of B16F10 cells, LF, and B16F10-CM-treated LF (Fig. 6a). CTSB was one of the proteins that was identified to be the most differentially expressed in the secretome of B16F10-CM-treated LF. Twelve distinct peptides that span the polypeptide sequences of CTSB were identified (Supplementary Figure S5a). As one of the most studied cysteine cathepsins, CTSB has been shown to be involved in tumor formation, growth, and invasion [19]. We next questioned whether CTSB contributed to fibroblast-promoted metastatic colonization. Western blotting was used to further investigate the secretion of CTSB. The results showed that CTSB was abundant in the CM from B16F10-CM-treated LF (Fig. 6b). To determine whether CTSB is responsible for fibroblast-mediated activation of PI3K/Akt/mTOR pathway in tumor cells, we used Z-FA-FMK, an irreversible CTSB inhibitor, to treat B16F10 cells in the coculture system. The inhibition of CTSB blocked the fibroblast-mediated activation of PI3K/Akt/mTOR pathway, as demonstrated by the decreased phosphorylations of Akt, mTOR, and S6K, compared with those in controls. Meanwhile, inhibition of CTSB also blocked fibroblast-induced expression of SREBP1 and SCD1 (Fig. 6c). Conversely, the treatment of CTSB induced the activation of PI3K/Akt/mTOR pathway and the expression of SREBP1 and SCD1 in B16F10 cells (Supplementary Figure S5b). Furthermore, the treatment of Z-FA-FMK reversed lung fibroblast-induced growth-promoting effect on tumor cells (Fig. 6d). On the other hand, the treatment of Z-FA-FMK, KU-006379, or LY294002 compromised lung fibroblast-increased oleic acid levels in tumor cells (Supplementary Figure S5c). In brief, these data strongly support the hypothesis that lung fibroblast-secreted

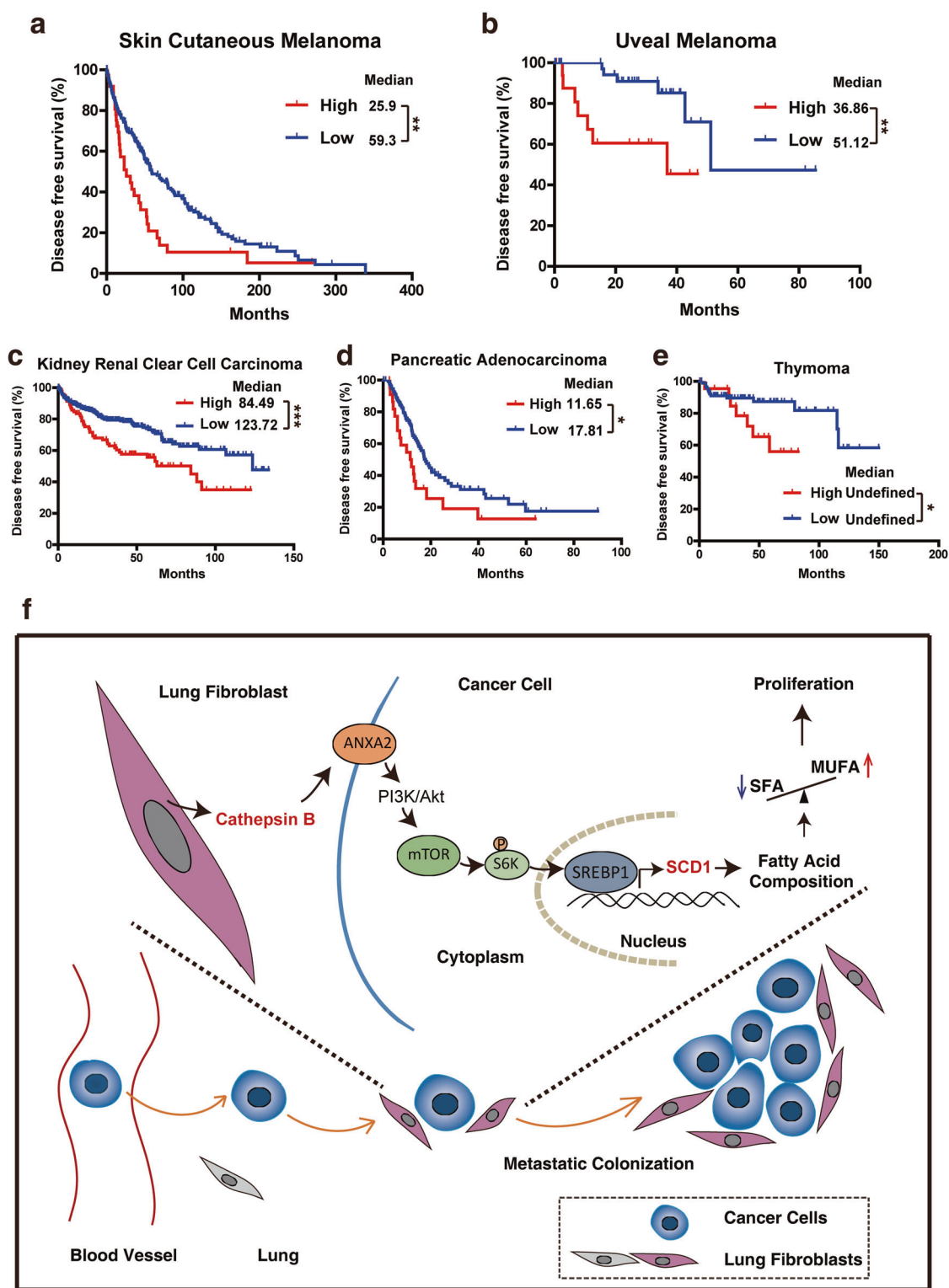


Fig. 7 High *SCD1* gene expression is associated with shorter disease-free survival in cancer patients. Kaplan–Meier disease-free survival (DFS) curves for the patients with skin cutaneous melanoma (**a**) and uveal melanoma (**b**), kidney renal clear cell carcinoma (**c**), pancreatic adenocarcinoma (**d**), and thymoma (**e**) based on *SCD1* expression in

TCGA dataset. The red line represents the DFS of patients with high *SCD1* expression level (mRNA expression z -scores > 0.5), and the blue line represents the DFS of patients with low *SCD1* expression level (mRNA expression z -scores < 0.5). Median survival time is undefined in (**e**). (**f**) Proposed model for lung fibroblasts promoted metastatic colonization. * $P < 0.05$, ** $P < 0.01$, *** $P < 0.001$

CTSB increased the expression of SCD1 in tumor cells through PI3K/Akt/mTOR pathway.

In addition to its extracellular proteases function, CTSB could also bind to cell surface receptors. We therefore asked which receptor mediates the CTSB-induced SCD1 overexpression. To answer this question, we tested whether the expression of SCD1 was influenced by transducing shRNAs targeting the cell surface proteins, which are associated with CTSB. The results showed that targeting *Anxa2* remarkably reduced the expression level of SCD1 (Supplementary Figure S5d). The transducing *Anxa2* shRNAs showed a significant reduction in the expression of ANXA2 both at mRNA and protein levels (Fig. 6e). Similarly, targeting *Anxa2* blocked the fibroblast-mediated activation of PI3K/Akt/mTOR pathway and the subsequent SREBP1 and SCD1 expressions (Fig. 6f). Meanwhile, targeting *Anxa2* also reversed lung fibroblast-mediated increase of tumor cell proliferation (Fig. 6g). Altogether, these data indicate that CTSB induces the expression of SCD1 in tumor cells through ANXA2.

Next, we performed an *in vivo* study to investigate whether inhibition of CTSB could suppress lung fibroblast-mediated promotion of metastatic colonization. We intravenously co-injected freshly isolated LF with B16F10 cells into mice and treated the mice with Z-FA-FMK once daily for 7 days. We found that Z-FA-FMK treatment significantly suppressed fibroblast-increased metastasis (Fig. 6h, i). Collectively, these data confirm that upregulation of SCD1 in tumor cells elicited by CTSB is an essential mechanism that mediates lung fibroblast-promoted metastatic colonization (Fig. 7f).

High SCD1 gene expression is associated with shorter DFS in cancer patients

To extend our study to human cancers, we analyzed SCD1 expression in melanoma patients in different stages. The clinical features of melanoma patient samples are shown in Supplementary Table 3. We observed increased SCD1 protein expression in lymph node metastatic melanoma compared with benign and primary malignant tumor (Supplementary Figure S6a). Meanwhile, the expression of SCD1 did not show significant difference among benign tumor and different stages of primary malignant tumor (Supplementary Figures S6b and c). In the B16F10 subcutaneous model, the expression of SCD1 was also increased in lung metastasis compared with B16F10 primary tumor (Supplementary Figures S6d and e). These findings demonstrate that SCD1 is mainly upregulated in tumor cells at distant organs.

We also examined the clinical significance of *SCD1* expression among skin cutaneous melanoma and other four cancer types at the mRNA level using TCGA datasets.

Patients were stratified as either *SCD1* high or low expression. Patients with high *SCD1* expression displayed significantly shorter DFS than the rest of patients in skin cutaneous melanoma ($P = 0.0043$, Fig. 7a). Interestingly, survival analyses also revealed a link between increased *SCD1* expression level and shorter DFS among uveal melanoma ($P = 0.0056$, Fig. 7b), kidney renal clear cell carcinoma ($P = 0.0009$, Fig. 7c), pancreatic adenocarcinoma ($P = 0.0289$, Fig. 7d), and thymoma ($P = 0.0432$, Fig. 7e). Taken together, these results illustrate that *SCD1* expression is clinically relevant in cancer patients, possibly linking *SCD1* expression with tumor progression.

Discussion

Emerging evidence suggests that the supportive stroma is critical for metastatic colonization of tumor cells in distant organs [7, 20, 21]. Our findings identify the initiation of melanoma lung metastasis via SCD1-induced fatty acid composition changes in tumor cells, which was mediated by fibroblast-secreted CTSB. Meanwhile, inhibition of SCD1 significantly suppressed lung metastasis and prolonged the overall survival of mice. We believe that targeting SCD1 offers an important therapeutic opportunity in preventing tumor metastasis.

Our previous studies suggested that certain factors expressed in LF, such as MMPs, angiotensin 2, and miR-30s, can influence the pulmonary vascular integrity in pre-metastatic phase [22, 23]. Other groups also found that fibroblast-secreted fibronectin makes lung a docking site for the subsequent arrived tumor cells [24]. In this work, our data demonstrate a critical role of LF in metastatic colonization, the time after tumor cells arrival. CTSB is frequently overexpressed in several types of cancer and correlated with a poor prognosis [25, 26]. Previous studies have suggested that CTSB plays multiple roles in tumor development, including initiation, proliferation, angiogenesis, invasion, and metastasis [27]. It is noteworthy that CTSB-deficient mice displayed reduced metastatic burden in the lungs [28]. Peters and colleagues also reported that macrophage-secreted CTSB enhanced the metastasis of mammary carcinomas to the lungs [29]. In addition to the roles of tumor cell-derived CTSB in tumor progression, these studies revealed that CTSB plays a vital role in crosstalk between tumor cells and stromal cells in tumor metastasis. Our results demonstrated that fibroblast-secreted CTSB facilitated metastatic colonization through the influences on SCD1 expression and subsequent fatty acid composition changes in tumor cells. In addition to CTSB, we also found other cysteine cathepsins, such as cathepsin L and cathepsin Z, were secreted by fibroblasts after B16F10-CM treatment in our mass spectrometry results (data not show). Due to the

important roles of cysteine cathepsins in different stages of tumor progression [19], it will be of great interest to investigate the specific mechanisms by which tumor–stromal interactions promote metastatic colonization through cysteine cathepsins.

In order to support rapid growth and proliferation, tumor cells must achieve high rates of fatty acid synthesis. During this process, mTOR signaling serves as a central regulator of lipid metabolism [10]. SREBP transcription factors are key regulators of lipogenic genes, including SCD1 [17]. It is well established that mTOR complex 1 (mTORC1) regulates lipogenesis by activating SREBPs in an S6K-dependent or S6K-independent manner [30, 31]. Meanwhile, mTOR complex 2 (mTORC2) also stimulates lipogenesis through Akt-mediated activation of SREBP1 [32, 33]. In this work, we found that cocultured with fibroblasts increased the phosphorylation level of S6K, which elevated the expression of SREBP1 and SCD1. SCD1 is a pivotal constituent in fatty acid metabolism which generates MUFAs from SFAs [34]. Apart from the important roles in lipid storage and obesity, MUFAs are key precursors of membrane phospholipids, triglycerides, and cholesterol esters. MUFAs are also involved in signal transduction which can stimulate tumor cell growth [35]. Our results demonstrated that the fatty acid composition in tumor cells was changed when cocultured with LF. A higher level of MUFA (oleic acid) and a lower level of SFAs (palmitic acid and stearic acid) were found in tumor cells cocultured with LF. It was reported that SFAs can induce cell apoptosis through the generation of ceramide and reactive intermediates. And the presence of SCD1 can prevent the lipotoxicity through the conversion of SFAs to MUFAs [36]. Accili's group recently have illustrated a shared mechanism of obesity and tumor progression mediated by the expression of SCD1 [37]. Huang and colleagues also proved that SCD1 is associated with tumor promotion and poor survival in lung adenocarcinoma [38]. Our studies provide deeper insights into how fatty acid composition influences metastatic colonization. The involvement of lipid metabolism in tumor progression is an intriguing issue which needs further investigation.

In addition to its influence on fatty acid composition, Copland's group showed that SCD1 supports tumor cell proliferation through induction of endoplasmic reticulum stress in clear cell renal cell carcinoma [13]. SCD1 is also reported to regulate autophagy-induced cell death and chemoresistance in hepatocellular carcinoma [39, 40]. Our work, for the first time, clarifies the importance of SCD1 in lung metastatic colonization. Both genetic knockdown and pharmacological inhibition of SCD1 compromised lung fibroblast-promoted metastasis and prolonged the overall survival of mice. These results provide further insights in understanding the role of LF in promoting metastatic

colonization. Notably, inhibition of SCD1 may target multiple signal pathways, with an extensive inhibitory effect on tumor metastasis.

In summary, our work identifies SCD1 as a key modulator of tumor cell proliferation that is activated by lung fibroblast-secreted CTSSB at the metastatic niche. Therefore, inhibition of CTSSB or SCD1 offers promising therapeutic approaches for the treatment of tumor metastasis.

Materials and methods

Cell culture, reagents, and antibodies

All melanoma cell lines (B16F10, A875, and A375), human fetal LF MRC5 and human embryonic kidney cell line HEK-293T were obtained from the American Type Culture Collection (Manassas, VA, USA). The isolation of murine LF were described in supplementary methods as previously mentioned [23]. Cells were maintained in Dulbecco's Modified Eagle's Medium supplemented with 10% fetal bovine serum and 1% antibiotics. Z-FA-FMK, KU-0063794, and LY294002 were from Selleck Chemical (Houston, TX, USA). CAY10566 and oleic acid were from Cayman (Ann Arbor, MI, USA). Palmitic acid was from Sigma-Aldrich (St. Louis, MO, USA). CTSSB was from Sino Biological Inc. (Beijing, China). Antibodies against p-Akt, Akt, p-mTOR, mTOR, p-S6K, S6K, p-S6, S6, and PCNA were from Cell Signaling Technology (Beverly, MA, USA). Antibodies against QPRT, CEP55, HSP90, β -actin, SREBP1, ANXA2, and CTSSB were from Abcam (Cambridge, UK). Antibodies against TAOK2 and CDK1 were from Bioworld Technology (Louis Park, MN, USA). Antibodies against SCD1, RAC3, PLTP, α -SMA, and RNF114 were from GeneTex (San Antonio, TX, USA).

Cell proliferation analysis

B16F10 cells (2×10^3 cells per well) were plated in 48-well plates and cultured for 24 h, then the upper chamber plated with LF (2×10^3 cells per chamber) was settled in the 48-well plates for coculture. Cell proliferation was determined using the colorimetric Cell Counting Kit-8 (CCK-8, Dojindo Laboratories, Kumamoto, Japan) after 72 h, as reported [41]. The concentrations of drugs and fatty acids were as follows: CAY10566, 10 μ M [42]; KU-0063794, 1 μ M [43]; LY294002, 10 μ M [44]; Z-FA-FMK, 10 μ M [45]; oleic acid, 25 μ M [11]; and palmitic acid, 50 μ M [46].

Gene expression analysis

B16F10 cells were cocultured with LF for 24 or 48 h. Total RNAs were extracted and the gene expression was

measured by qRT-PCR using a previously described protocol [47]. All primers used are listed in Supplementary Table 1.

Plasmids and cell transfection

HEK-293T were co-transfected with the packaging vector psPAX2, envelope plasmid pVSVG, and transfer plasmid SGEP [48] containing the shRNA species targeting *Scd1*. SGEP containing Ren.713 shRNA served as negative control as reported [48]. Following 72 h, the HEK-293T medium containing the virus was collected, filtered through an 0.45 μ M PVDF filter and transferred to B16F10 plate. The medium was replaced after 72 h and cells containing the integrated virus were selected with puromycin (50 ng/ μ l). shRNAs targeting *Anxa2*, *Tlr9*, *Itgb1*, *Igfbp7*, *Plaur*, and *Fgfr2* were purchased from Sigma-Aldrich (St. Louis, MO, USA). Sequences of all the shRNAs used are listed in Supplementary Table 1

Fatty acid composition analysis

Cell lipids were extracted using the Lipid Extraction Kit from BioVision (Milpitas, CA, USA) and were esterified with methanol. Fatty acid methyl esters were analyzed for fatty acid composition by ISQTM GC-MS system (Thermo Scientific, TX, USA). The detailed analytical conditions are described in supplementary methods.

Liquid chromatography-tandem mass spectrometry

For identification of lung fibroblast-secreted factors in coculture system, conditioned medium from B16F10, LF, or B16F10-CM-treated LF were separated by SDS-PAGE. The differential bands were analyzed by liquid chromatography-tandem mass spectrometry (LC-MS/MS), as previously described [49]. The detailed analytical conditions are described in supplementary methods.

Animal studies

All animal studies were approved by the Institutional Animal Care and Use Committee of Tsinghua University (project numbers: 13-LYZ2 and 17-LYZ1). B16F10 cells (1×10^5 per mouse) with or without freshly isolated LF (1×10^5 per mouse) were intravenously injected from C57BL/6 mice (6 weeks of age) tail vein. Then, mice were treated with CAY10566 (2.5 mg/kg) [50] or Z-FA-FMK (1 mg/kg) [51] for 7 days. Lung metastasis was detected 21 days after cell injection. A375 cells (1×10^5 per mouse) with or without MRC5 cells (1×10^5 per mouse) were intravenously injected from BALB/c nude mice (6 weeks of

age) tail vein. Lung metastasis was detected 49 days after cell injection. Lung sections were stained with haematoxylin and eosin. The lung metastasis areas were measured with Image Pro Plus (Media Cybernetics). The investigator was blinded during the experiments.

Survival analysis of TCGA datasets

The publicly available cBioPortal for Cancer Genomics (<http://www.cbioportal.org/>) [52, 53] and The Cancer Genome Atlas (TCGA) datasets were utilized to analyze *SCD1* gene expression and DFS in five types of cancer.

Statistical analysis

The samples were allocated to experimental groups in a completely random design. All experiments were performed in triplicates whenever applicable. The sample size and the significance analysis are specified in figure legends. Data were presented as mean \pm SD except for pulmonary metastasis data, which were expressed as mean \pm SEM. Statistical significance of differences was assessed by two-tailed Student's *t*-test. Survival analysis was assessed by Mantel-Cox log-rank test. A value of $P < 0.05$ was considered significant compared with controls.

Funding

This work was supported in part by the General Programs of the National Natural Science Foundation of China (Nos. 81672865, 81472667, 81461148021, and 81272529) and the Major Scientific and Technological Special Project for "significant new drugs creation" (No. 2013ZX09509103).

Acknowledgements We thank Zhirui Yang (Peking University) for assistance in drawing schematic diagram and Yang Chen (MD Anderson Cancer Center) for assistance in manuscript preparation.

Compliance with ethical standards

Conflict of interest The authors declare that they have no competing interests.

References

1. Siegel RL, Miller KD, Jemal A. Cancer statistics, 2016. *CA Cancer J Clin.* 2016;66:7–30.
2. Gray-Schopfer V, Wellbrock C, Marais R. Melanoma biology and new targeted therapy. *Nature.* 2007;445:851–7.
3. Vanharanta S, Massague J. Origins of metastatic traits. *Cancer Cell.* 2013;24:410–21.
4. Malanchi I, Santamaria-Martinez A, Susanto E, Peng H, Lehr HA, Delaloye JF, et al. Interactions between cancer stem cells and their niche govern metastatic colonization. *Nature.* 2012;481:85–89.

5. Chen Q, Zhang XH, Massague J. Macrophage binding to receptor VCAM-1 transmits survival signals in breast cancer cells that invade the lungs. *Cancer Cell*. 2011;20:538–49.
6. Wculek SK, Malanchi I. Neutrophils support lung colonization of metastasis-initiating breast cancer cells. *Nature*. 2015;528:413–7.
7. Miranda F, Mannion D, Liu S, Zheng Y, Mangala LS, Redondo C, et al. Salt-inducible kinase 2 couples ovarian cancer cell metabolism with survival at the adipocyte-rich metastatic niche. *Cancer Cell*. 2016;30:273–89.
8. Kalluri R, Zeisberg M. Fibroblasts in cancer. *Nat Rev Cancer*. 2006;6:392–401.
9. Igal RA. Stearoyl CoA desaturase-1: new insights into a central regulator of cancer metabolism. *Biochim Biophys Acta-Mol Cell Biol Lipids*. 2016;1861:1865–80.
10. Luyimbazi D, Akcakanat A, McAuliffe PF, Zhang L, Singh G, Gonzalez-Angulo AM, et al. Rapamycin regulates stearoyl CoA desaturase 1 expression in breast cancer. *Mol Cancer Ther*. 2010;9:2770–84.
11. Du X, Wang QR, Chan E, Merchant M, Liu J, French D, et al. FGFR3 stimulates stearoyl CoA desaturase 1 activity to promote bladder tumor growth. *Cancer Res*. 2012;72:5843–55.
12. Noto A, Raffa S, De Vitis C, Roscilli G, Malpicci D, Coluccia P, et al. Stearoyl-CoA desaturase-1 is a key factor for lung cancer-initiating cells. *Cell Death Dis*. 2013;4:e947.
13. von Roemeling CA, Marlow LA, Wei JJ, Cooper SJ, Caulfield TR, Wu K, et al. Stearoyl-CoA desaturase 1 is a novel molecular therapeutic target for clear cell renal cell carcinoma. *Clin Cancer Res*. 2013;19:2368–80.
14. Fritz V, Benfodda Z, Rodier G, Henriquet C, Iborra F, Avances C, et al. Abrogation of de novo lipogenesis by stearoyl-CoA desaturase 1 inhibition interferes with oncogenic signaling and blocks prostate cancer progression in mice. *Mol Cancer Ther*. 2010;9:1740–54.
15. Wang J, Xu Y, Zhu L, Zou Y, Kong W, Dong B, et al. High expression of stearoyl-CoA desaturase 1 predicts poor prognosis in patients with clear-cell renal cell carcinoma. *PLoS One*. 2016;11:e0166231.
16. Mamane Y, Petroulakis E, LeBacquer O, Sonenberg N. mTOR, translation initiation and cancer. *Oncogene*. 2006;25:6416–22.
17. Ricoult SJ, Manning BD. The multifaceted role of mTORC1 in the control of lipid metabolism. *EMBO Rep*. 2013;14:242–51.
18. Lewis CA, Brault C, Peck B, Bensaad K, Griffiths B, Mitter R, et al. SREBP maintains lipid biosynthesis and viability of cancer cells under lipid- and oxygen-deprived conditions and defines a gene signature associated with poor survival in glioblastoma multiforme. *Oncogene*. 2015;34:5128–40.
19. Mohamed MM, Sloane BF. Cysteine cathepsins: multifunctional enzymes in cancer. *Nat Rev Cancer*. 2006;6:764–75.
20. Wu JB, Yin L, Shi C, Li Q, Duan P, Huang JM, et al. MAOA-dependent activation of Shh-IL6-RANKL signaling network promotes prostate cancer metastasis by engaging tumor-stromal cell interactions. *Cancer Cell*. 2017;31:368–82.
21. Liu G, Chen Y, Qi F, Jia L, Lu XA, He T, et al. Specific chemotherapeutic agents induce metastatic behaviour through stromal- and tumour-derived cytokine and angiogenic factor signalling. *J Pathol*. 2015;237:190–202.
22. Huang Y, Song N, Ding Y, Yuan S, Li X, Cai H, et al. Pulmonary vascular destabilization in the premetastatic phase facilitates lung metastasis. *Cancer Res*. 2009;69:7529–37.
23. Qi F, He T, Jia L, Song N, Guo L, Ma X, et al. The miR-30 family inhibits pulmonary vascular hyperpermeability in the premetastatic phase by direct targeting of Skp2. *Clin Cancer Res*. 2015;21:3071–80.
24. Quail DF, Joyce JA. Microenvironmental regulation of tumor progression and metastasis. *Nat Med*. 2013;19:1423–37.
25. Harbeck N, Alt U, Berger U, Krüger A, Thomssen C, Jänicke F, et al. Prognostic impact of proteolytic factors (urokinase-type plasminogen activator, plasminogen activator inhibitor 1, and cathepsins B, D, and L) in primary breast cancer reflects effects of adjuvant systemic therapy. *Clin Cancer Res*. 2001;7:2757–64.
26. Jedeszko C, Sloane BF. Cysteine cathepsins in human cancer. *Biol Chem*. 2004;385:1017–27.
27. Aggarwal N, Sloane BF. Cathepsin B: multiple roles in cancer. *Proteom Clin Appl*. 2014;8:427–37.
28. Vasiljeva O, Korovin M, Gajda M, Brodoefel H, Bojic L, Kruger A, et al. Reduced tumour cell proliferation and delayed development of high-grade mammary carcinomas in cathepsin B-deficient mice. *Oncogene*. 2008;27:4191–9.
29. Vasiljeva O, Papazoglou A, Kruger A, Brodoefel H, Korovin M, Deussing J, et al. Tumor cell-derived and macrophage-derived cathepsin B promotes progression and lung metastasis of mammary cancer. *Cancer Res*. 2006;66:5242–50.
30. Duvel K, Yecies JL, Menon S, Raman P, Lipovsky AI, Souza AL, et al. Activation of a metabolic gene regulatory network downstream of mTOR complex 1. *Mol Cell*. 2010;39:171–83.
31. Porstmann T, Santos CR, Griffiths B, Cully M, Wu M, Leever S, et al. SREBP activity is regulated by mTORC1 and contributes to Akt-dependent cell growth. *Cell Metab*. 2008;8:224–36.
32. Shimobayashi M, Hall MN. Making new contacts: the mTOR network in metabolism and signalling crosstalk. *Nat Rev Mol Cell Biol*. 2014;15:155–62.
33. Hagiwara A, Cornu M, Cybulski N, Polak P, Betz C, Trapani F, et al. Hepatic mTORC2 activates glycolysis and lipogenesis through Akt, glucokinase, and SREBP1c. *Cell Metab*. 2012;15:725–38.
34. Igal RA. Stearoyl-CoA desaturase-1: a novel key player in the mechanisms of cell proliferation, programmed cell death and transformation to cancer. *Carcinogenesis*. 2010;31:1509–15.
35. Atilla-Gokcumen GE, Muro E, Relat-Goberna J, Sasse S, Bedigian A, Coughlin ML, et al. Dividing cells regulate their lipid composition and localization. *Cell*. 2014;156:428–39.
36. Listenberger LL, Han X, Lewis SE, Cases S, Farese RV Jr, Ory DS, et al. Triglyceride accumulation protects against fatty acid-induced lipotoxicity. *Proc Natl Acad Sci USA*. 2003;100:3077–82.
37. Qiang L, Kon N, Zhao W, Jiang L, Knight Colette M, Welch C, et al. Hepatic SirT1-dependent gain of function of stearoyl-CoA desaturase-1 conveys dysmetabolic and tumor progression functions. *Cell Rep*. 2015;11:1797–808.
38. Huang J, Fan XX, He J, Pan H, Li RZ, Huang L, et al. SCD1 is associated with tumor promotion, late stage and poor survival in lung adenocarcinoma. *Oncotarget*. 2016;7:39970.
39. Huang GM, Jiang QH, Cai C, Qu M, Shen W. SCD1 negatively regulates autophagy-induced cell death in human hepatocellular carcinoma through inactivation of the AMPK signaling pathway. *Cancer Lett*. 2015;358:180–90.
40. Bansal S, Berk M, Alkhouri N, Partrick DA, Fung JJ, Feldstein A. Stearoyl-CoA desaturase plays an important role in proliferation and chemoresistance in human hepatocellular carcinoma. *J Surg Res*. 2014;186:29–38.
41. Chen Y, Liu G, Guo L, Wang H, Fu Y, Luo Y. Enhancement of tumor uptake and therapeutic efficacy of EGFR-targeted antibody cetuximab and antibody-drug conjugates by cholesterol sequestration. *Int J Cancer*. 2015;136:182–94.
42. AbuAli G, Chaisaklert W, Stelloo E, Pazarentzos E, Hwang MS, Qize D, et al. The anticancer gene ORCTL3 targets stearoyl-CoA desaturase-1 for tumour-specific apoptosis. *Oncogene*. 2014;34:1718–28.

43. Nodomi S, Umeda K, Saida S, Kinehara T, Hamabata T, Daifu T, et al. CD146 is a novel marker for highly tumorigenic cells and a potential therapeutic target in malignant rhabdoid tumor. *Oncogene*. 2016;35:5317–27.
44. Zhang L, Zhang W, Li Y, Alvarez A, Li Z, Wang Y, et al. SHP-2-upregulated ZEB1 is important for PDGFRalpha-driven glioma epithelial-mesenchymal transition and invasion in mice and humans. *Oncogene*. 2016;35:5641–52.
45. Oberle C, Huai J, Reinheckel T, Tacke M, Rassner M, Ekert PG, et al. Lysosomal membrane permeabilization and cathepsin release is a Bax/Bak-dependent, amplifying event of apoptosis in fibroblasts and monocytes. *Cell Death Differ*. 2010;17:1167–78.
46. Roy D, Mondal S, Wang C, He X, Khurana A, Giri S, et al. Loss of HSulf-1 promotes altered lipid metabolism in ovarian cancer. *Cancer Metab*. 2014;2:13–13.
47. Jia L, Lu XA, Liu G, Wang S, Xu M, Tian Y, et al. Endostatin sensitizes p53-deficient non-small-cell lung cancer to genotoxic chemotherapy by targeting DNA-dependent protein kinase catalytic subunit. *J Pathol*. 2017;243:255–66.
48. Fellmann C, Hoffmann T, Sridhar V, Hopfgartner B, Muhar M, Roth M, et al. An optimized microRNA backbone for effective single-copy RNAi. *Cell Rep*. 2013;5:1704–13.
49. Wang H, Chen Y, Lu XA, Liu G, Fu Y, Luo Y. Endostatin prevents dietary-induced obesity by inhibiting adipogenesis and angiogenesis. *Diabetes*. 2015;64:2442.
50. Kamphorst JJ, Cross JR, Fan J, de Stanchina E, Mathew R, White EP, et al. Hypoxic and Ras-transformed cells support growth by scavenging unsaturated fatty acids from lysophospholipids. *Proc Natl Acad Sci*. 2013;110:8882–7.
51. Kim M, Hansen KK, Davis L, van Marle G, Gill MJ, Fox JD, et al. Z-FA-FMK as a novel potent inhibitor of reovirus pathogenesis and oncolysis in vivo. *Antivir Ther*. 2010;15:897.
52. Cerami E, Gao J, Dogrusoz U, Gross BE, Sumer SO, Aksoy BA, et al. The cBio cancer genomics portal: an open platform for exploring multidimensional cancer genomics data. *Cancer Discov*. 2012;2:401–4.
53. Gao J, Aksoy BA, Dogrusoz U, Dresdner G, Gross B, Sumer SO, et al. Integrative analysis of complex cancer genomics and clinical profiles using the cBioPortal. *Sci Signal*. 2013;6:p11.